BJC

Genistein suppresses aerobic glycolysis and induces hepatocellular carcinoma cell death

Sainan Li[1], Jingjing Li[1], Weiqi Dai[1], Qinghui Zhang[2], Jiao Feng[1], Liwei Wu[1], Tong Liu[1], Qiang Yu[3], Shizan Xu[3], Wenwen Wang[1], Xiya Lu[1], Kan Chen[1], Yujing Xia[1], Jie Lu[1], Yingqun Zhou[1], Xiaoming Fan[4], Wenhui Mo[5], Ling Xu*,[6] and Chuanyong Guo*,[1]

[1]Department of Gastroenterology, Shanghai Tenth People's Hospital, Tongji University School of Medicine, Shanghai 200072, China; [2]Department of Clinical Laboratory, Kunshan First People's Hospital Affiliated to Jiangsu University, Kunshan, JiangSu 215300, China; [3]Department of Gastroenterology, Shanghai Tenth Hospital, School of Clinical Medicine of Nanjing Medical University, Shanghai 200072, China; [4]Department of Gastroenterology, Jinshan Hospital of Fudan University, Jinshan, Shanghai 201508, China; [5]Department of Gastroenterology, Minhang Hospital, Fudan University, Shanghai 201100, China and [6]Department of Gastroenterology, Shanghai Tongren Hospital, Shanghai Jiao Tong University School of Medicine, Shanghai 200336, China

Background: Genistein is a natural isoflavone with many health benefits, including antitumour effects. Increased hypoxia-inducible factor 1 α (HIF-1α) levels and glycolysis in tumour cells are associated with an increased risk of mortality, cancer progression, and resistance to therapy. However, the effect of genistein on HIF-1α and glycolysis in hepatocellular carcinoma (HCC) is still unclear.

Methods: Cell viability, apoptosis rate, lactate production, and glucose uptake were measured in HCC cell lines with genistein incubation. Lentivirus-expressed glucose transporter 1 (GLUT1) or/and hexokinase 2 (HK2) and siRNA of HIF-1α were used to test the direct target of genistein. Subcutaneous xenograft mouse models were used to measure *in vivo* efficacy of genistein and its combination with sorafenib.

Results: Genistein inhibited aerobic glycolysis and induced mitochondrial apoptosis in HCC cells. Neither inhibitors nor overexpression of HK2 or GLUTs enhance or alleviate this effect. Although stabiliser of HIF-1α reversed the effect of genistein, genistein no longer has effects on HIF-1α siRNA knockdown HCC cells. In addition, genistein enhanced the antitumour effect of sorafenib in sorafenib-resistant HCC cells and HCC-bearing mice.

Conclusions: Genistein sensitised aerobic glycolytic HCC cells to apoptosis by directly downregulating HIF-1α, therefore inactivating GLUT1 and HK2 to suppress aerobic glycolysis. The inhibitory effect of genistein on tumour cell growth and glycolysis may help identify effective treatments for HCC patients at advanced stages.

Hepatocellular carcinoma (HCC) is associated with high mortality rates and its malignance is highly related to the metabolic change in HCC cells (Iansante *et al*, 2015). Glucose metabolism in HCC cells is characterised by two major biochemical events: increased glucose uptake and aerobic glycolysis. The former is strongly dependent on the upregulated expression and activity of glucose transporters (GLUTs), which are 10–12-fold higher in tumours than in healthy cells (Mueckler and Thorens, 2013). GLUT1, the expression of which is regulated by hypoxia-inducible factor 1 α (HIF-1α), is considered the main overexpressed isoform in a wide range of human cancers (Barron *et al*, 2016). Hexokinase (HK) 2, which catalyses the first rate-limiting step of glycolysis (Vander Heiden *et al*, 2009), is the only one that retains catalytic capacity in both C- and N-terminal portions to double the rate of glycolysis (Lis *et al*, 2016). In addition, instead of

being free in the cytosol, HK2 is frequently located strategically within the outer mitochondrial membrane and binds to transmembrane voltage-dependent anion channels (VDACs; Mazure, 2017), to block the release of cytochrome c (Cyt c) from mitochondria, thus protecting cancer cells from apoptosis. These features may explain why the overexpression of HK2 or/and GLUTI can be considered as a typical feature of the malignant phenotype. Agents targeting these molecules may provide a potential therapeutic option for advanced HCC.

Genistein (Gen), a soybean-derived isoflavonoid compound, produced almost exclusively in leguminous species, has been studied extensively for its health benefits (Jeong et al, 2004; Xu et al, 2009). The blood concentration of Gen in individuals varies markedly depending on soy consumption: it is 100–1000 times higher in high-soy-diet Asian consumers than in low-soy-diet Western consumers, and the differences have been linked to various clinical outcomes (Adlercreutz et al, 1993). Population-based studies suggest that the plasma Gen level is inversely associated with the risk of several types of cancers, especially breast, endometrial, and prostate neoplasms (Kurahashi et al, 2008; Shike et al, 2014). Gen exhibits antitumour activities through various mechanisms, such as oestrogenic activity (Gertz et al, 2012), antioxidant (Zhou and Liu, 2013; Wang et al, 2017), anti-migration (Dai et al, 2015a), and metabolism regulation (Vera et al, 1996). Studies have shown its apoptosis induction effect in aerobic glycolytic HCC cells (Wang et al, 2014). However, the mechanism underlying the effect of Gen, especially its role in glucose metabolism, is not fully understood.

In the present study, we showed that Gen inhibited glycolysis and induced apoptosis in HCC cells. Further investigation showed that Gen inhibited the expression and activity of HIF-1α to suppress GLUT1/HK2. In addition, Gen improved the sensitivity to sorafenib (Sora) in Sora-resistant HCC cells with activated glycolysis in vitro and in vivo, providing evidence for its potential clinical application in the treatment of HCC.

MATERIALS AND METHODS

Reagents. Gen, glucose, 3-bromopyruvate (3-BP), roxadustat (FG-4592), and cytochalasin B (CB) were purchased from Sigma-Aldrich (St Louis, MO, USA). Sora tosylate was purchased from Selleck (Selleck Chemicals, Shanghai, China), and dissolved in dimethyl sulfoxide (Sigma-Aldrich).

Cell culture. Five human HCC cell lines (HCC-LM3, SMMC-7721, Hep3B, Bel-7402, and Huh-7) and a normal hepatic cell line (LO2; Dai et al, 2014) were purchased from Chinese Academy of Sciences Committee Type Culture Collection cell bank and cultured in high-glucose Dulbecco's modified Eagle's medium (Hyclone, Logan, UT, USA) supplemented with 10% foetal bovine serum, $100\,U\,ml^{-1}$ penicillin, and $100\,mg\,ml^{-1}$ streptomycin at $37\,°C$ in a humidified atmosphere of 5% CO_2.

Cell viability test. CCK-8 solution ($10\,\mu l$; Peptide Institute Inc., Osaka, Japan) was added to cells in a 96-well plate. The plate was maintained in a dark incubator ($37\,°C$, 5% CO_2) for 2 h, and then absorbance was measured at 450 nm using a microplate reader for further half maximal inhibitory concentration (IC_{50}) analysis.

Apoptosis analysis and JC-1 staining. Cells were stained with propidium iodide (PI)-Annexin V/fluorescein isothiocyanate or phycoerythrin-Annexin V/7-amino-actinomycin (BD BioSciences, San Jose, CA, USA) according to the manufacturer's instructions. JC-1 ($10\,\mu g\,ml^{-1}$; BD BioSciences) was used to measure mitochondrial membrane potential. Cells were then analysed using a flow cytometer (Cytomics FC500; Beckman Coulter, Fullerton, CA, USA).

Cell cycle analysis. Cells were treated with Gen and were fixed with cold 70% ethanol overnight. After washing once with PBS, cells were stained with PI (BD BioSciences) and analysed on a flow cytometer.

Biochemical assays. To measure 2-DG uptake, cells were washed with uptake buffer twice, cultured in $1\,\mu Ci\,ml^{-1}$ [^{3}H]-2-DG at $37\,°C$ for 30 min, and solubilised with 0.1% sodium dodecyl sulfate (SDS). The radioactivity was calculated using a liquid scintillation counter, normalised to the protein content, and corrected for the zero-time uptake per mg protein. Lactate levels were measured using a fluorometric assay (BioVision, Milpitas, CA, USA). O_2 consumption was tested using the 110 Fiber optic oxygen monitor (Instech, Plymouth Meeting, PA, USA) and expressed as nmol O_2 per million cells per min. ATP content was measured with an ATP detection kit according to the manufacturer's instructions (Promega, Madison, AL, USA). HK, PFK, PK activity, and NADPH/NADP Quantitation were measured using detection kits according to the manufacturer's instructions (Sigma-Aldrich). Transcription activity of HIF-1α was detected using TransAM HIF-1 Transcription Factor ELISA Kits (Active Motif, Carlsbad, CA, USA) according to the manufacturer's protocol.

Reverse transcription PCR and quantitative real-time–PCR. The TRIzol reagent was used to extract total RNA. cDNA was synthesised using SuperScript II reverse transcriptase with Oligo (dT; Invitrogen, Carlsbad, CA, USA). The real-time PCR experiment was performed following the protocol of the real-time PCR kit (Takara, Dalian, China). The levels of the target genes were normalised to β-actin.

Protein extraction and western blotting. The cytosolic and mitochondrial fractions were separated and purified using a Mitochondrial Isolation Kit (Pierce, Rockford, IL, USA) according to the manufacturer's protocol. Total cellular proteins were extracted using radioimmunoprecipitation assay buffer (Sigma-Aldrich) containing protease inhibitors. The samples were then resolved by SDS-polyacrylamide gel electrophoresis and transferred to polyvinyl difluoride membranes. The membranes were sequentially blocked in PBS containing 0.1% Tween 20 (PBST) with 5% non-fat milk for 1 h and probed with primary antibodies (Cell Signaling Technology, Danvers, MA, USA), and then washed with PBST three times and incubated with appropriate secondary antibodies for 1 h at room temperature. Finally, the membranes were washed again and scanned using the Odyssey two-colour infrared laser imaging system (LI-COR Biosciences, Lincoln, NE, USA). β-actin was used as an internal control.

Plasmid construction, lentivirus packaging, and infection. Full-length cDNAs encoding the GLUT1 or HK2 or GLUT1/HK2 sequence were amplified from 293 T cDNA and then cloned into the pCDH-CMV-MCS-EF1-GFP vectors (System Biosciences, Mountain View, CA, USA). Empty lentiviral vector was used as control. HCC-LM3 cells were infected with empty vector or lentivirus-expressed target genes in the presence of $8\,\mu g\,ml^{-1}$ polybrene (Sigma-Aldrich) overnight.

HIF-1α expression in HCC-LM3 cells was ablated with siRNAs. Scramble siRNA (scRNA) was used as control. All plasmid sequences were confirmed by DNA sequencing. The siRNAs were transfected into cells using Lipofectamine 2000 (Invitrogen). The transduction efficiency was measured by real-time PCR and western blotting.

Animal experiments. Four-week-old male athymic BALB/C nu/nu mice with free access to water and food were housed in a standard animal laboratory with a 12-h light–dark cycle and constant environmental conditions. All experiments were performed in accordance with ethical standards and in compliance with the Declaration of Helsinki, and according to the national and

international guidelines. The study was approved by the Animal Care and Use Committee of Shanghai Tongji University. Serum-free culture medium (200 μl) containing HCC-LM3 cells (5×10^6) was subcutaneously injected into the upper flank region of 24 mice. When the tumour volume was $\sim 100 \, mm^3$, the animals were randomly divided into four groups: normal control (NC), and Gen (20, 40, and 80 mg kg^{-1}) according to previous publications (Qin et al, 2015). Saline or Gen was given by oral gavage once a day for 21 days. Tumour volume was calculated using the following formula: volume (mm^3) = (width)^2 × length/2. Body weight of mice was measured every 4 days. Mice were killed 24 h after the last treatment. Tumours were resected and imaged using a high-definition digital camera. Haematoxylin and eosin (HE) were used to stain the nuclear region and cytoplasm to observe histopathology changes. The terminal deoxynucleotidyl transferase-mediated dUTP nick-end labelling (TUNEL) assay was used to measure the extent of tumour cell apoptosis, and the percentage of TUNEL-positive cells was determined by counting the average number of cells under four high-power fields. Protein expression of GLUT1 and HK2 was detected using immunohistochemistry.

For the combination treatment, another 24 mice that received upper flank injection of HCC-LM3 cells were divided into four groups: NC, Sora alone (10 mg kg^{-1}), Gen alone (40 mg kg^{-1}), and combination treatment (Sora 10 mg kg^{-1} + Gen 40 mg kg^{-1}; Dai et al, 2015b; Li et al, 2016). Both Sora and Gen were given by oral gavage once a day for 30 days. Measurements were performed as described above.

Statistical analysis. All results are expressed as means ± s.d. Statistical analysis was performed using a two-tailed unpaired Student's t-test and SPSS 17.0 software (IBM, Armonk, NY, USA). Quantitative data are representative of at least three independent experiments. Values of *$P < 0.05$, **$P < 0.01$, and ***$P < 0.001$ were considered statistically significant.

RESULTS

Gen inhibited proliferation, caused cell cycle arrest at the G2/M phase, and induced apoptosis and autophagy in HCC cells in vitro. Gen inhibited cell viability in a time- and dose-dependent manner in all HCC cell lines (Figure 1A and B). The IC$_{50}$ of Gen for cell proliferation inhibition in HCC-LM3, Bel-7402, Huh-7, Hep3B, SMMC-7721, and LO2 cells was 67.31, 71.44, 103.53, 92.71, 86.47, and 161.41 μM, respectively, at 48 h. The protein expression of proliferating cell nuclear antigen (PCNA) confirmed the effect of Gen on inhibiting cell growth (Figure 1C). The normal liver cell line LO2 was barely affected at a certain concentration range of Gen (Figure 1A and B), suggesting that Gen can inhibit cancer cells without markedly affecting normal cells.

Gen causes cell cycle arrest at the G2/M phase in various types of cancer cells (Fang et al, 2016). Incubation with Gen significantly increased the proportion of cells in the G2/M phase in HCC-LM3 and Bel-7402 cells, concomitant with a decrease in the number of cells in the G0/G1 phase (Figure 1D).

Treatment with Gen significantly induced apoptosis in HCC-LM3 cells (Figure 1E). In Bel-7402 cells, the apoptosis rate with Gen treatment at 40 μM was slightly higher than that in untreated cells, although the difference did not reach statistical significance ($P = 0.061$). Gen at 60 and 80 μM significantly induced apoptosis in Bel-7402 cells (Figure 1E). Consistent with the apoptosis staining results, there was a significant increase in protein expression of active caspases 3 and 9 and a decrease in cleaved poly ADP-ribose polymerase (PARP) in both HCC cell lines treated with Gen (Figure 1C). These results indicated that Gen induced apoptosis in HCC cells in vitro.

In addition, Gen at 60 and 80 μM induced the expression of biomarkers of autophagy, LC3-II and Beclin1 (Figure 1C), indicating that, besides apoptosis, Gen also induced autophagy in aerobic glycolytic HCC cells.

Gen inhibited HCC cell growth in vivo. Mice treated with Gen at 40 and 80 mg kg^{-1} showed a significantly smaller tumour size than those treated with saline (Figure 1F). Mice treated with Gen at 20 mg kg^{-1} did not differ significantly from the control group, showing a small reduction in tumour size (0.462 ± 0.036 vs 0.891 ± 0.195, $P = 0.074$). The results of dynamic observations of the antitumour effects of Gen treatment for 21 days showed the same pattern (Supplementary Figure S1A).

Nuclear fragmentation in HE staining with Gen treatment suggested a considerable degree of necrosis (Figure 1G). No significant body weight loss or liver, kidney, lung, and spleen damage were observed during the 21 days of treatment (Supplementary Figure S1B and C), demonstrating the safety of Gen in vivo.

Gen inhibited glycolysis in aerobic glycolytic HCC cell lines. HCC-LM3 and Bel-7402 possess higher glycolysis rate and higher expression of GLUT1 and HK2 (Supplementary Figure S2), consistent with previous report (Dai et al, 2015b), can be viewed as typical high-glycolytic cells. Gen decreased lactate concentration in HCC-LM3 and Bel-7402 cells in a dose-dependent manner, and the pattern of glucose uptake was similar to that of lactate production (Figure 2A and B), indicating that Gen inhibited aerobic glycolysis in HCC cells. With Gen treatment at 40 μM for 24 h, ATP generation from glycolysis has already been inhibited in HCC-LM3 and Bel-7402 cells, whereas the slightest inhibition on oxidative phosphorylation did not happen until the drug concentration reached 120 μM (Supplementary Figure S3), suggesting that Gen suppressed energy production mainly depending on the inhibition of glycolysis.

Gen treatment at 80 μM for 12 h caused an $\sim 50\%$ reduction in the glycolysis rate compared with that in untreated cells (Figure 2A). However, cell proliferation was not obviously affected under the same conditions (Figure 1B). A similar decrease in the glycolysis rate without an obvious inhibition of cell proliferation was observed in response to Gen at 40 μM for 24 h (Figures 1A and 2B). These results indicated that the effect of Gen on suppressing glycolysis occurs before its effect on cell growth inhibition (earlier time and smaller dosage).

Among all tested key glycolytic enzymes, HK2 was the most downregulated enzyme at the mRNA level in both HCC cells treated with 60 μM Gen for 24 h (Figure 2C), closely followed by GLUT1. Western blot analysis showed that Gen treatment for 24 h significantly downregulated the protein expression of HK2 (both total and mitochondria-bound HK2) and GLUT1 in a dose-dependent manner (Figure 2D). Immunohistochemical staining showed that Gen treatment downregulated GLUT1 and HK2 in xenograft tumours in vivo (Figure 2E), suggesting that the cytotoxicity of Gen correlates with decreased expression of GLUT1 and HK2.

What is noteworthy is that Gen treatment impaired the activities of HK, PFK, and PK (Supplementary Figure S4A–C), albeit to varying degrees, although the mRNA expression of PFKs and PKM2 was not inhibited significantly. In addition, the elevated ratio of NADPH/NADP suggested a shunt to the pentose phosphate pathway (Supplementary Figure S4D), indicating that with the aerobic glycolysis pathway suppressed, the biosynthetic pathway (i.e., pentose phosphate pathway) was motivated to generate nucleotides, amino acids, and so on.

GLUT1 and HK2 are not directly involved in the effect of Gen on HCC cells. Treatment with 50 and 100 mM glucose
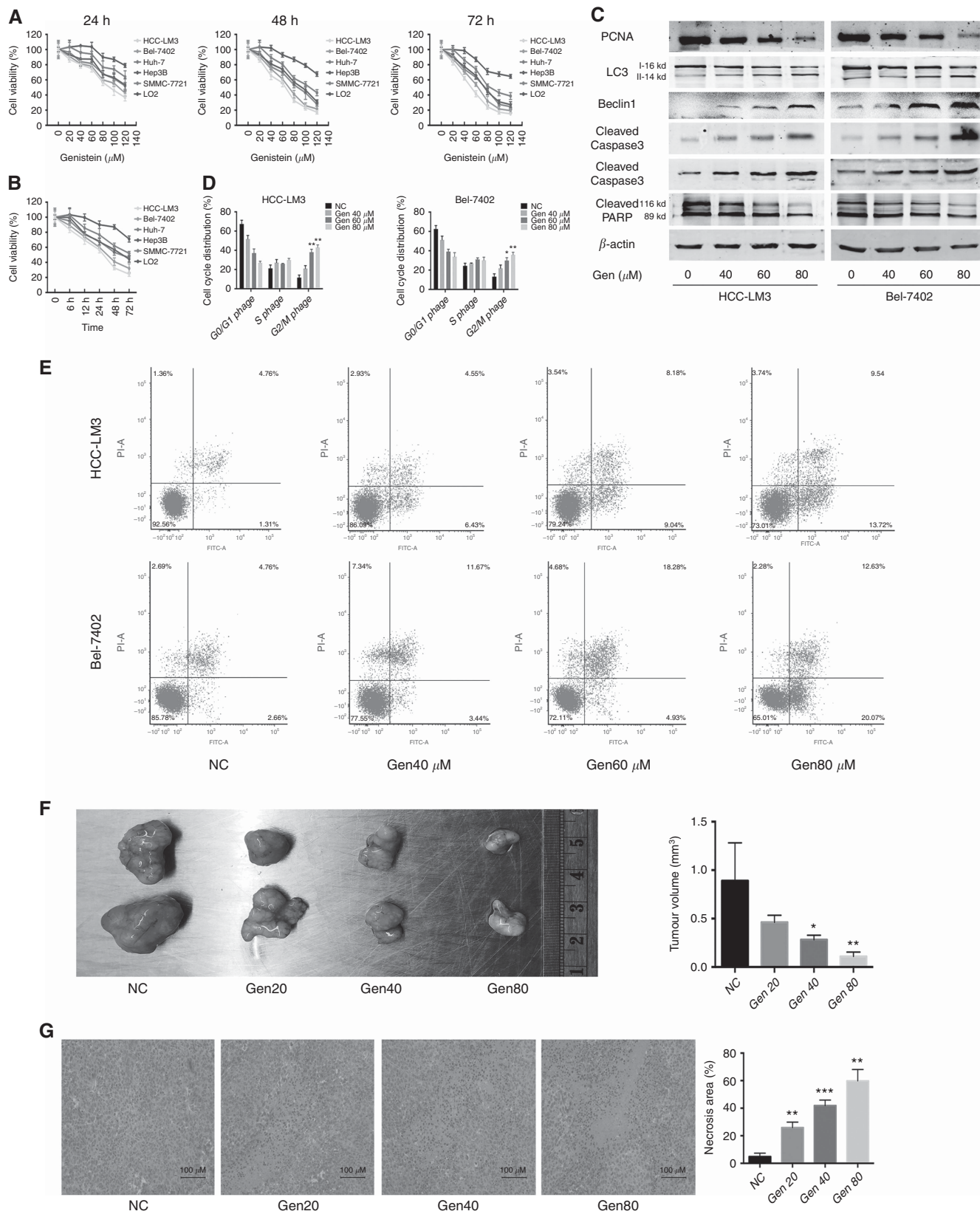
Figure 1. Genistein inhibits HCC cell growth *in vitro* and *in vivo*. (**A**, **B**) Cell viability of LO2 and five HCC cells treated with genistein (Gen, 0–80 μM) for 24, 48, or 72 h (**A**), or genistein 80 μM for 6–72 h (**B**). (**C**) The protein levels of PCNA, LC3, Beclin1, cleaved-caspase 3/9, and PARP in HCC cells treated with genistein for 48 h. β-actin was used as a loading control. (**D**) Genistein incubation for 48 h induced cell cycle arrest in HCC-LM3 and Bel-7402 cells. (**E**) Genistein incubation for 48 h induced apoptosis in HCC-LM3 and Bel-7402 cells. (**F**, **G**) In a xenograft mouse model, mice were treated with genistein (0, 20, 40, or 80 mg kg^{-1}) for 21 days. At the time points indicated, the following measurements were performed: diameter of tumours (**F**), and the per cent of HE-positive tumour cells (**G**). Plotted values represent the mean ± s.e of three independent experiments. *$P < 0.05$, **$P < 0.01$, ***$P < 0.001$.

significantly reversed the Gen-induced suppression of cell proliferation and apoptosis induction in HCC-LM3 cells (Figure 3A–C), suggesting that glucose transport was involved in

Gen-induced HCC-LM3 cell death. However, CB, a glucose transporter inhibitor (Wu *et al*, 2009), had no effect on the inhibition of cell proliferation or activation of apoptosis induced by
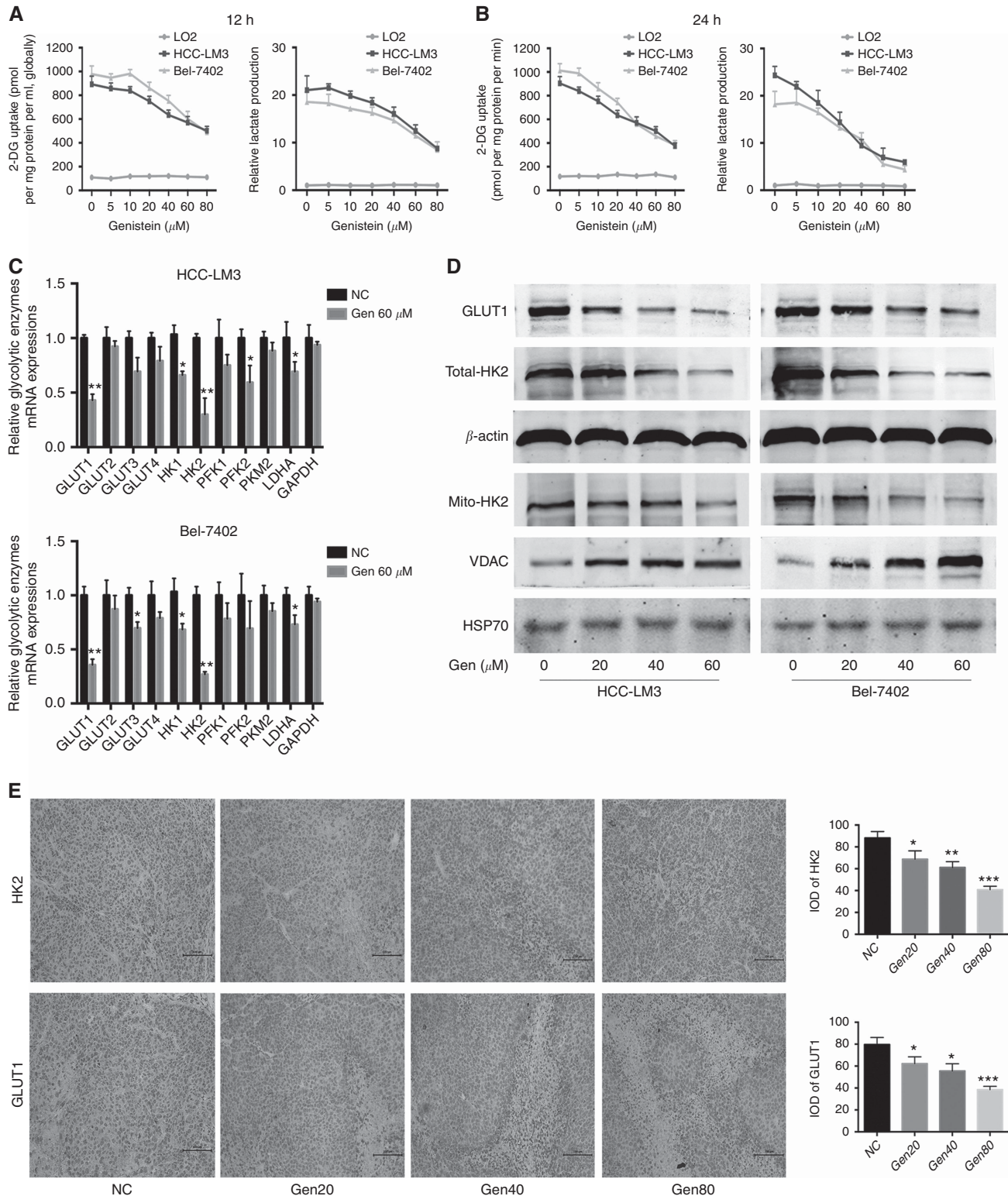

Figure 2. Genistein inhibits glycolysis in aerobic glycolytic HCC cell lines. (**A**, **B**) Relative lactate production and 2-DG uptake from HCC-LM3, Bel-7402, and LO2 cells treated with genistein (0–80 μM) for 12 h (**A**) or 24 h (**B**). (**C**) qRT–PCR analysis of the effect of genistein (60 μM) for 24 h on the expression of genes associated with glycolysis in HCC cells. (**D**) Protein expression of GLUT1, total- and mito-HK2, and VDAC in HCC cells incubated with genistein for 24 h. β-actin and HSP-70 were used as loading controls. (**E**) Immunohistochemical staining and its integral optical density (IOD) for HK2 and GLUT1 in tumours in the xenograft mouse model. Plotted values represent the mean ± s.e. of three independent experiments. *$P < 0.05$, **$P < 0.01$, ***$P < 0.001$.
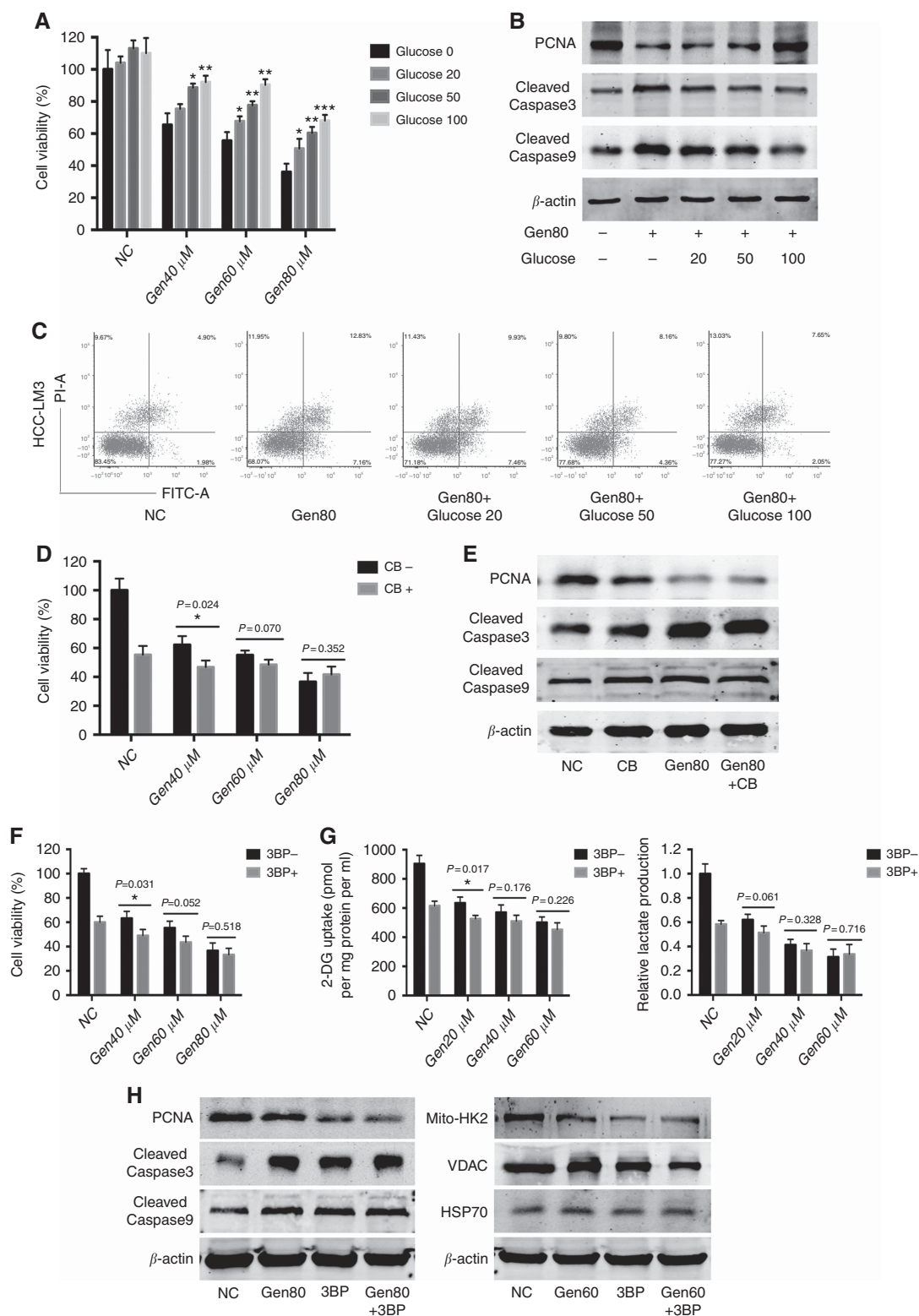
Figure 3. Extra glucose reversed the effect of genistein on HCC cells, whereas CB and 3-BP had no obvious effect. (**A**) Cell viability of HCC-LM3 cells treated with genistein and glucose for 48 h. (**B**) Western blot analysis of PCNA and cleaved-caspase 3/9 in HCC-LM3 cells treated with genistein and glucose for 48 h. β-actin was used as a loading control. (**C**) Apoptosis rate of HCC-LM3 cells treated with genistein and glucose for 48 h. (**D**) Cell viability of HCC-LM3 cells incubated for 48 h with genistein with or without CB (20 μM). (**E**) Western blot analysis of PCNA and cleaved-caspase 3/9 in HCC-LM3 cells treated with genistein or/and CB (20 μM) for 48 h. β-actin was used as a loading control. (**F**) Cell viability of HCC-LM3 cells treated with genistein with or without 3-BP (100 μM) for 48 h. (**G**) Relative lactate production and 2-DG uptake in HCC-LM3 cells treated with genistein with or without 3-BP (100 μM) for 24 h. (**H**) Western blot analysis of PCNA, cleaved-caspase 3, and PARP in HCC-LM3 cells treated with genistein or/and 3-BP (100 μM) for 48 h, and mito-HK2 and VDAC in HCC-LM3 cells treated with genistein or/and 3-BP (100 μM) for 24 h. β-actin and HSP-70 were used as loading controls. Plotted values represent the mean ± s.e. of three independent experiments. *$P < 0.05$, **$P < 0.01$, ***$P < 0.001$.

Gen (Figure 3D and E). In addition, 3-BP, a direct HK2 inhibitor (Guo *et al*, 2016), did not enhance or abolish the proliferation-inhibitory effect of Gen (Figure 3F and H). A similar pattern was observed in glucose uptake, lactate production, and mitochondrial HK2 expression in aerobic glycolytic HCC cells (Figure 3G and H).
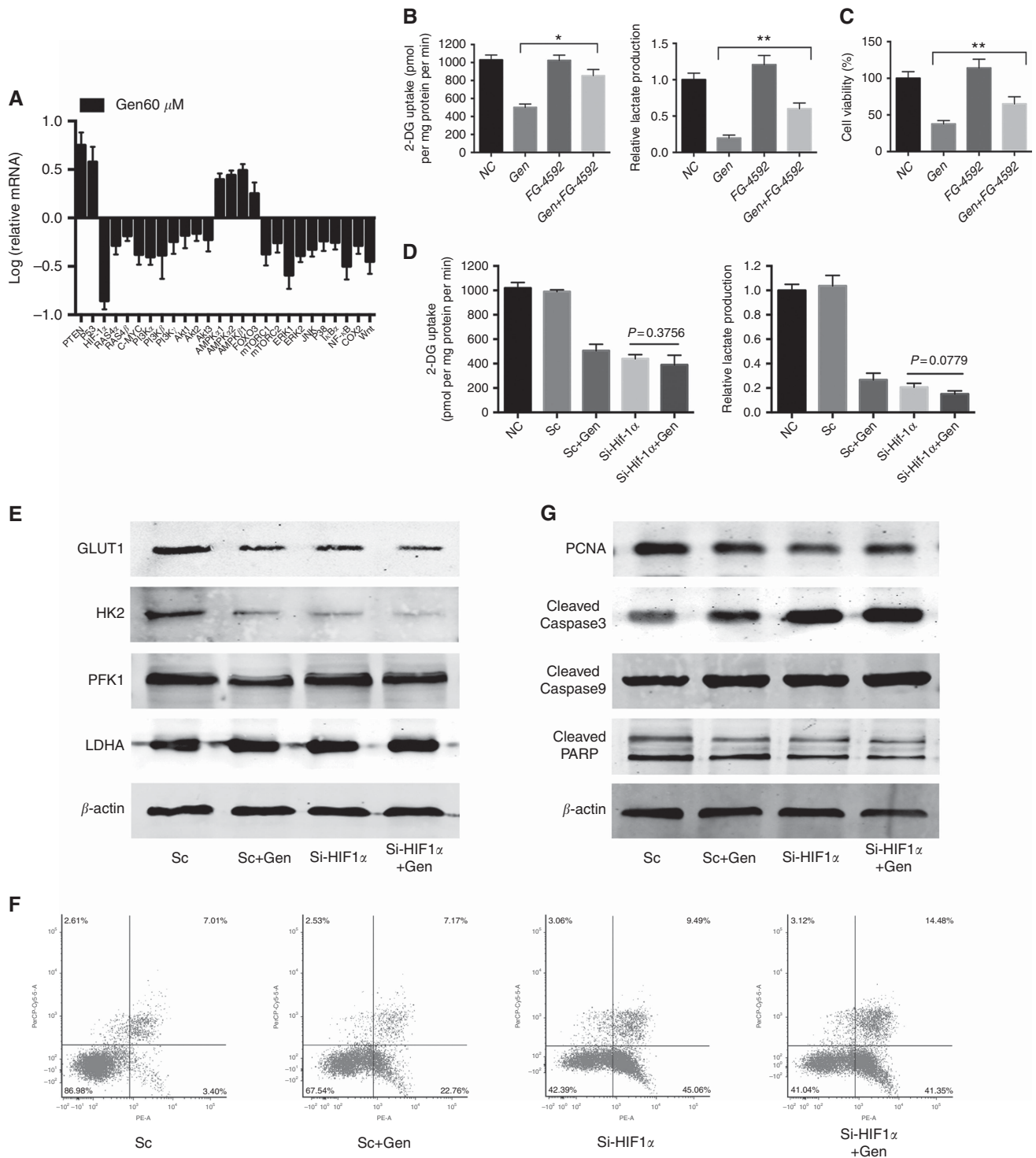

Figure 4. HIF-1α is dominant in the genistein-suppressed HCC glycolysis and proliferation. (**A**) qRT–PCR analysis of the effect of genistein (60 μM) for 24 h on the expression of genes associated with both glycolysis and apoptosis in HCC-LM3 cells. (**B**) Relative lactate production and 2-DG uptake in HCC-LM3 cells incubated in genistein (60 μM) or/and FG-4592 (25 μM) for 24 h. (**C**) Cell viability of HCC-LM3 cells incubated in genistein (80 μM) or/and FG-4592 (25 μM) for 48 h. (**D**) Relative lactate production and 2-DG uptake in HIF-1α siRNA (Si) or scramble RNA (Sc) transfected HCC-LM3 cells with or without genistein (60 μM) for 24 h. (**E**) Western blot analysis of the expression of GLUT1, HK2, PFK1, and lactate dehydrogenase A (LDHA) in HIF-1α-Si or Sc HCC-LM3 cells with or without genistein (60 μM) for 24 h. β-actin was used as a loading control. (**F**) After HIF-1α siRNA or scramble RNA transfection, HCC-LM3 cells were treated with or without genistein (80 μM) for 48 h to monitor cell apoptosis rate. (**G**) Western blot analysis of PCNA, and cleaved-caspase. 3/9, and PARP in HIF-1α si or Sc HCC-LM3 cells treated with or without genistein (80 μM) for 48 h. β-actin was used as a loading control. Plotted values represent the mean ± s.e. of three independent experiments. *$P < 0.05$, **$P < 0.01$.
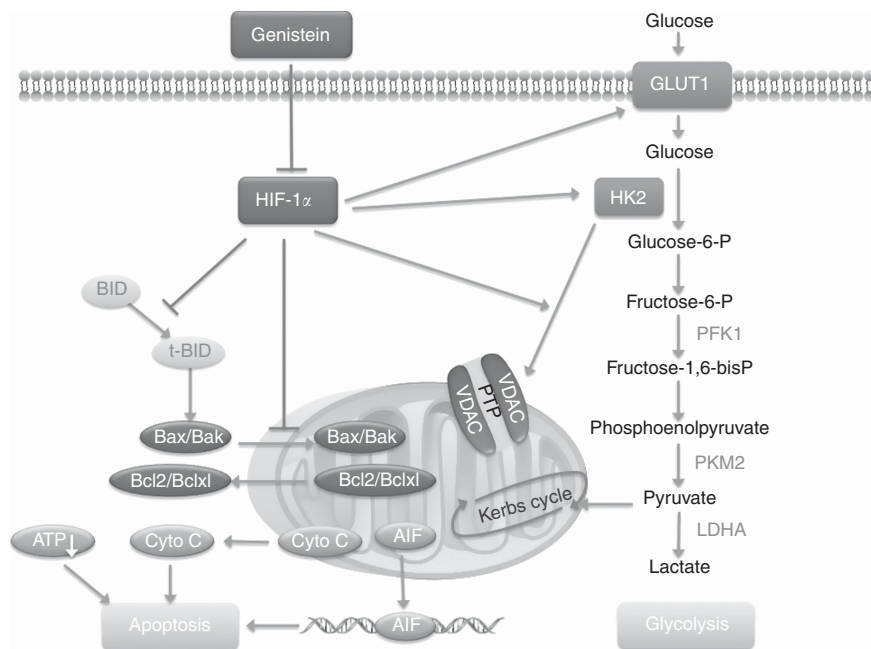
Figure 5. Mechanism of genistein-mediated inhibition of glycolysis and induction of apoptosis in HCC cells. Inhibition of HIF1-α by genistein led to the suppression of high GLUT1 and HK2 expression in sorafenib-resistant HCC cells, resulting in the suppression of ATP production. In addition, disruption of the HK2/VDAC complex led to mitochondrial membrane potential loss, resulting in cell death. Inhibition of HIF1-α activated the pro-apoptotic proteins Bax and Bak, as well as the cleavage of Bid, which interacts with the anti-apoptotic Bcl-2 family proteins Bcl-2 and Bcl-xl to relieve their apoptosis-inhibitory effect. Apoptogenic substrates were thus released from the mitochondria, such as cytochrome c into the cytoplasm and apoptosis-inducing factor (AIF) to the nucleus, causing caspase activation and cell apoptosis, and therefore restoring the sensitivity to sorafenib.

Inhibitors of HK2 or GLUTs did not enhance or alleviate the effect of Gen, which led us to speculate that this phenomenon may be attributed to one of the two following reasons: first, when 3-BP inhibits HK2 activity and CB binds to GLUT1, there is no target for Gen, and its inhibitory effect on glycolysis and cell growth is abolished; second, GLUT1 and HK2 are not directly involved in the antitumour effect of Gen.

To test which hypothesis was correct, we overexpressed GLUT1 or/and HK2 in HCC-LM3 cells (Supplementary Figure S5A). All clones grew at similar rates with Gen treatment (Supplementary Figure S5B). No statistically significant differences in the rate of inhibition of glucose uptake or lactate production by Gen were observed among the four clones (Supplementary Figure S5C). Overexpression of GLUT1 and/or HK2 did not affect Gen-induced cell growth or glycolysis inhibition, indicating that the second hypothesis was correct: GLUT1 and HK2 are not directly involved in the antitumour effect of Gen.

Gen-inhibited glycolysis and HCC cell growth are dependent on the suppression of HIF-1α. Among all 26 tested metabolic regulation pathways, HIF-1α showed the greatest alteration (decreased by 84%; Figure 4A) with Gen treatment. Protein expression and transcription activity of HIF-1α was also inhibited by Gen in a dose-dependent manner (Supplementary Figure S6). Roxadustat, a prolyl-4-hydroxylase inhibitor and HIF-1α stabiliser (Hoppe *et al*, 2016), reversed the glycolysis inhibitory effect of Gen (Figure 4B) and attenuated Gen-inhibited HCC cell proliferation (Figure 4C). These results suggested that HIF-1α is involved in the Gen-suppressed HCC glycolysis and proliferation.

Glucose uptake and lactate production were decreased in HIF-1α siRNA knockdown HCC-LM3 cells (Figure 4D and Supplementary Figure S7), and this effect was not enhanced by treatment with Gen, suggesting that without the target HIF-1α the effect of Gen on glycolysis was abolished. In addition, the downregulated expression of the GLUT1 and HK2 proteins in HIF-1α siRNA knockdown cells was not decreased further with the addition of Gen (Figure 4E), indicating that the Gen-induced inhibition of GLUT1 and HK2 was dependent on the suppression of HIF-1α. By contrast, HIF-1α siRNA knockdown cells showed no obvious changes in the expression of phosphofructokinase (PFK) 1 and lactate dehydrogenase A (Figure 4E), suggesting that in the process of glycolysis regulation the specific downstream targets of HIF-1α were GLUT1 and HK2, but not other glycolytic enzymes.

Moreover, the apoptosis rate in HIF-1α siRNA knockdown cells was significantly increased compared with that in scRNA cells (Figure 4F). The addition of Gen in HIF-1α siRNA cells did not enhance the effect on apoptosis. The results of western blot analysis of PCNA, caspases, and PARP were consistent with the changes in apoptosis (Figure 4G), suggesting a direct involvement of HIF-1α in Gen-induced glycolysis inhibition and cell death.

In addition, Gen also reduced hypoxia-induced HIF-1α expression and enhanced hypoxic-cell death (Supplementary Figure S8), indicating this natural compound takes effect under both normal and hypoxic conditions.

Crosstalk between Gen-induced metabolic regulation and cell death machinery. Gen decreased the mitochondrial inner trans-membrane potential ($\Delta\psi$m) in a concentration-dependent manner (Supplementary Figure S9A), indicating an alteration of mitochondrial outer membrane permeabilisation (MOMP). It results in the release of apoptogenic factors such as Cyto c and apoptosis-inducing factor (Supplementary Figure S9B), which causes caspase 3/9 activation, leading to mitochondrial apoptosis.

Bcl-2 homology domain 3 proteins, such as truncated Bid, which are inhibited by HIF-1α (Guo *et al*, 2015), promote apoptosis by activating Bax/Bak (transferred from the cytosol to mitochondria) and inactivating Bcl-2/Bcl-xL to increase MOMP (Supplementary Figure S9B). Gen effectively blocked this process (Figure 5 and Supplementary Figure S9). Moreover, oxidative phosphorylation was inhibited by Gen at 80 and 120 μM (Supplementary Figure S9C), suggesting that energy deprivation (reduced ATP production) may also contribute to mitochondrial apoptosis. In addition, Gen induced
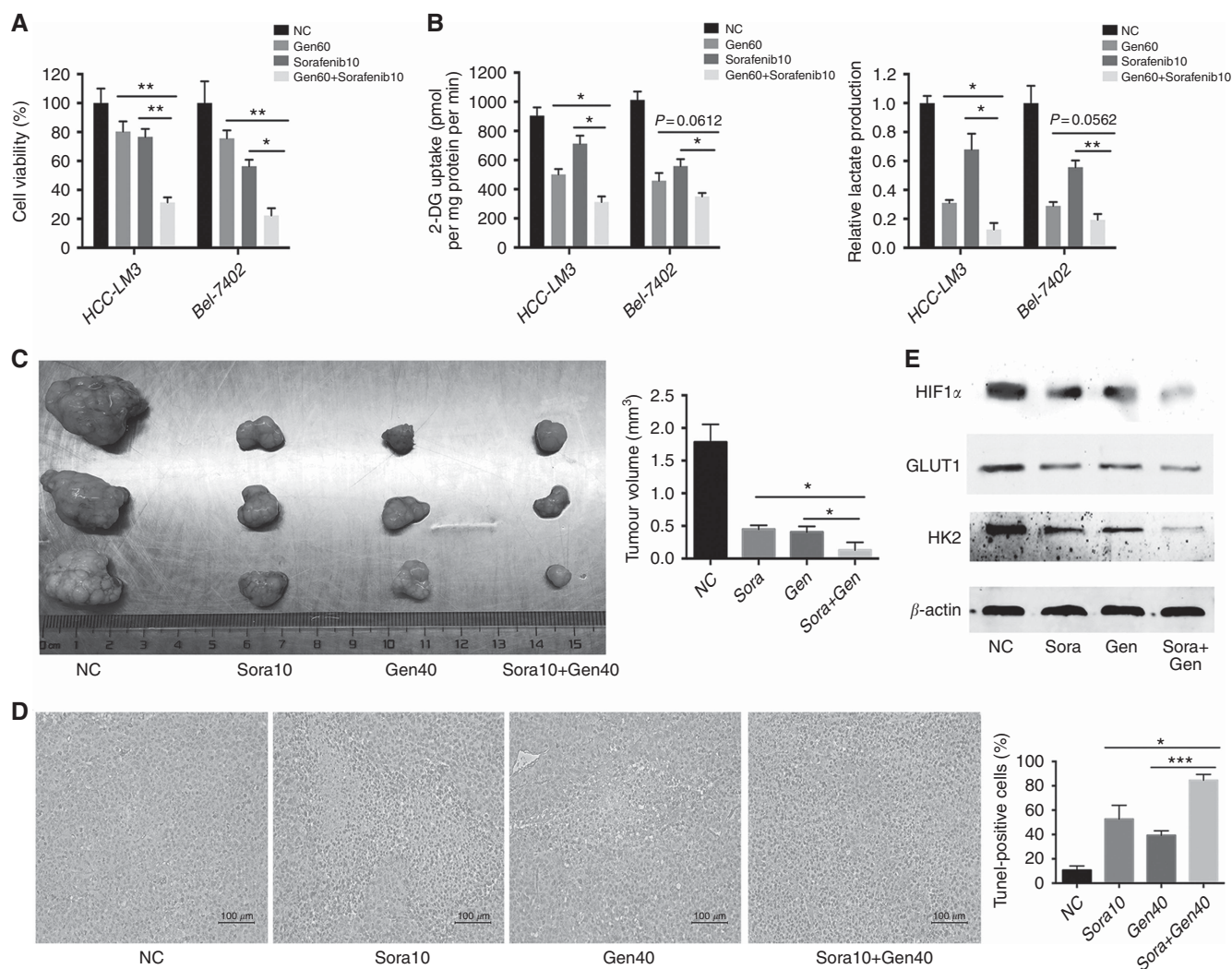
Figure 6. Genistein enhances sorafenib-induced cell growth inhibition in sorafenib-resistant HCC cells. (A, B) HCC-LM3 and Bel-7402 cells were exposed to genistein (60 μM) or/and sorafenib (10 μM) for 24 h, and cell viability (A), relative lactate production, and 2-DG uptake (B) were analysed. (C–E) In a xenograft mouse model, mice were treated with sorafenib (10 mg kg^{-1}) or/and genistein (40 mg kg^{-1}) for 30 days. At the time points indicated, the following measurements were performed: diameter of tumours (C), the percent of TUNEL-positive tumour cells (D), and protein expression of HIF-1α, GLUT1, and HK2 (E). Plotted values represent the mean ± s.e. of three independent experiments. *$P < 0.05$, **$P < 0.01$, ***$P < 0.001$.

the dissociation of HK2 from VDAC (Figure 2D), causing mitochondrial apoptosis through a different process.

Gen enhances Sora-induced cell growth inhibition in Sora-resistant HCC cells. HCC-LM3 and Bel-7402 cells, as typical Sora-resistant HCC cell lines (Dai *et al*, 2015b), showed IC$_{50}$ values for Sora of 15.78 and 12.17 μM at 24 h, respectively (Supplementary Figure S10), and were used for the combination treatment study. In HCC cells treated with Gen at 60 μM for 24 h, glycolysis was inhibited significantly, whereas cell proliferation was not obviously altered; treatment with Sora at 10 μM for 24 h significantly inhibited cell proliferation but not glycolysis rate (Figure 6A and B). However, combination treatment suppressed both proliferation and glycolysis rate, indicating an enhancement of both glycolysis and proliferation inhibition.

After 30 days of treatment with Gen (40 mg kg^{-1}) or/and Sora (10 mg kg^{-1}), tumour size in a mouse xenograft model was significantly smaller in the combination treatment group than in the Sora-alone or Gen-alone group (Figure 6C and Supplementary Figure 11A). Apoptosis rates in the TUNEL assay showed the opposite pattern (Figure 6D), without a significant effect on body

weight or vital organ function (Supplementary Figure 11B and C). HIF-1α, GLUT1, and HK2 expression was downregulated by combination treatment *in vivo* (Figure 6E), further indicating that Gen inhibited glycolysis and restored the sensitivity of Sora-resistant HCC cells to Sora treatment.

DISCUSSION

In the present study, we showed that Gen had a significant inhibitory effect on the growth of HCC cells, whereas it had little effect on normal liver cells (Figure 1). Gen induced apoptosis in aerobic glycolytic HCC cells, especially mitochondrial apoptosis, by regulating the Bcl-2 family proteins to increase MOMP and activate caspases (Supplementary Figure S9). In addition, Gen inhibited glycolysis in aerobic glycolytic HCC cells (Figures 2 and 5). Gen treatment at 40 μM for 24 h or 80 μM for 12 h significantly inhibited glycolysis, whereas there was no significant suppression of cell proliferation or apoptosis promotion, suggesting that glycolysis inhibition by Gen in high-glycolytic HCC cells occurs

before the inhibition of cell growth and apoptosis induction (smaller dose and earlier time).

Despite the fact that GLUT1 and HK2 showed the greatest reduction in response to Gen treatment, neither GLUT1 nor HK2 was the direct target of Gen. Evidenced by: first, the inhibitors of HK2 or GLUTs did not enhance or alleviate the inhibitory effect of Gen on glycolysis and apoptosis (Figure 3); and second, over-expression of GLUT1 or/and HK2 did not affect Gen-induced growth and glycolysis inhibition (Supplementary Figure S5).

Therefore, we identified the direct target of Gen. Among 26 cell growth and metabolic regulatory molecules, HIF-1α showed the greatest decrease in response to Gen treatment (Figure 4). The HIF-1α stabiliser reversed the glycolysis and viability inhibitory effect of Gen, and Gen had no obvious effect on HIF-1α-siRNA knockdown HCC cells, suggesting a direct involvement of HIF-1α in the effect of Gen on the inhibition of HCC cell growth and glycolysis.

HIFs are essential for tumour cells to adapt to a low-oxygen environment, as the oxygen supply is usually insufficient for the excessive growth of tumour cells (Semenza, 2013). Activated HIF-1α in tumour cells promotes cell survival through several mechanisms: first, it increases the expression and activity of glycolytic enzymes such as GLUT1 and HK2 to accelerate the glycolytic rate (Jain *et al*, 2016), thus meeting the energy demand of rapidly growing tumour cells; second, HIF-1α prevents tumour cell apoptosis by regulating Bcl-2 family proteins such as Bax and Bid (Erler *et al*, 2004), or stabilising the HK2/VDAC complex to avoid apoptosis; third, HIF-1α regulates autophagy by activating the *Bcl-2/E1B-19K interacting protein 3* (*Bnip3*) gene (Chinnadurai *et al*, 2008); and fourth, the interaction of HIF-1α and mutant onco- or anti-oncogenes such as P-53 and c-Myc also suppresses cell death (Zhang *et al*, 2007). Because HIF-1α mediates metabolic alterations and tumour cell death through many processes, our finding that the direct inhibition of HIF-1α by Gen results in suppressed glycolysis and enhanced apoptosis is not a surprise.

The role of aerobic glycolysis as a potential predictive biomarker of Sora resistance in HCC cells has been reported extensively (Shen *et al*, 2013; Li *et al*, 2016). Given the unique characteristics of Gen observed in the present study, including the inhibition of glycolysis at low doses and earlier times without an obvious effect on apoptosis, we therefore investigated whether Gen can be used to overcome Sora resistance. Combination treatment markedly suppressed both proliferation and glycolysis rate (Figure 6). Furthermore, Gen enhanced the ability of Sora to reduce the size of tumours and increase the apoptotic area in hepatoma-bearing nude mice through the inhibition of HIF-1α/GLUT1/HK2. These findings are in agreement with previous studies showing that Gen can enhance the sensitivity to tamoxifen in mammary cancer (Zhang *et al*, 2017), cisplatin in ovarian cancer (Arzuman *et al*, 2015), and methotrexate in leukaemia cells (Liu *et al*, 2015), providing preclinical evidence of the potential value of Gen for the treatment of HCC.

To the best of our knowledge, the present study is the first to investigate the mechanism underlying the effect of Gen on glycolysis mediated by the inhibition of HIF-1α/GLUT1/HK2 in HCC cells both *in vitro* and *in vivo*. In addition, this study is the first to demonstrate the enhancing effect and safety of combination treatment with Gen and Sora, providing a potential treatment strategy for Sora-resistant HCC patients. Further clinical trials are necessary to determine the drug dose, application start time, and duration in HCC patients.

CONFLICT OF INTEREST

The authors declare no conflict of interest.

REFERENCES

Adlercreutz H, Markkanen H, Watanabe S (1993) Plasma concentrations of phyto-oestrogens in Japanese men. *Lancet* **342**: 1209–1210.

Arzuman L, Beale P, Proschogo N, Yu JQ, Huq F (2015) Combination of genistein and cisplatin with two designed monofunctional platinum agents in human ovarian tumour Models. *Anticancer Res* **35**: 6027–6039.

Barron CC, Bilan PJ, Tsakiridis T, Tsiani E (2016) Facilitative glucose transporters: implications for cancer detection, prognosis and treatment. *Metabolism* **65**: 124–139.

Chinnadurai G, Vijayalingam S, Gibson SB (2008) BNIP3 subfamily BH3-only proteins: mitochondrial stress sensors in normal and pathological functions. *Oncogene* **27**(Suppl 1): S114–S127.

Dai W, Wang C, Wang F, Wang Y, Shen M, Chen K, Cheng P, Zhang Y, Yang J, Zhu R, Zhang H, Li J, Zheng Y, Lu J, Zhou Y, Xu L, Guo C (2014) Anti-miR-197 inhibits migration in HCC cells by targeting KAI 1/CD82. *Biochem Biophys Res Commun* **446**: 541–548.

Dai W, Wang F, He L, Lin C, Wu S, Chen P, Zhang Y, Shen M, Wu D, Wang C, Lu J, Zhou Y, Xu X, Xu L, Guo C (2015a) Genistein inhibits hepatocellular carcinoma cell migration by reversing the epithelial-mesenchymal transition: partial mediation by the transcription factor NFAT1. *Mol Carcinog* **54**: 301–311.

Dai W, Wang F, Lu J, Xia Y, He L, Chen K, Li J, Li S, Liu T, Zheng Y, Wang J, Lu W, Zhou Y, Yin Q, Abudumijiti H, Chen R, Zhang R, Zhou L, Zhou Z, Zhu R, Yang J, Wang C, Zhang H, Zhou Y, Xu L, Guo C (2015b) By reducing hexokinase 2, resveratrol induces apoptosis in HCC cells addicted to aerobic glycolysis and inhibits tumor growth in mice. *Oncotarget* **6**: 13703–13717.

Erler JT, Cawthorne CJ, Williams KJ, Koritzinsky M, Wouters BG, Wilson C, Miller C, Demonacos C, Stratford IJ, Dive C (2004) Hypoxia-mediated down-regulation of Bid and Bax in tumors occurs via hypoxia-inducible factor 1-dependent and -independent mechanisms and contributes to drug resistance. *Mol Cell Biol* **24**: 2875–2889.

Fang Y, Zhang Q, Wang X, Yang X, Wang X, Huang Z, Jiao Y, Wang J (2016) Quantitative phosphoproteomics reveals genistein as a modulator of cell cycle and DNA damage response pathways in triple-negative breast cancer cells. *Int J Oncol* **48**: 1016–1028.

Gertz J, Reddy TE, Varley KE, Garabedian MJ, Myers RM (2012) Genistein and bisphenol A exposure cause estrogen receptor 1 to bind thousands of sites in a cell type-specific manner. *Genome Res* **22**: 2153–2162.

Guo W, Zhang Y, Ling Z, Liu X, Zhao X, Yuan Z, Nie C, Wei Y (2015) Caspase-3 feedback loop enhances Bid-induced AIF/endoG and Bak activation in Bax and p53-independent manner. *Cell Death Dis* **6**: e1919.

Guo X, Zhang X, Wang T, Xian S, Lu Y (2016) 3-Bromopyruvate and sodium citrate induce apoptosis in human gastric cancer cell line MGC-803 by inhibiting glycolysis and promoting mitochondria-regulated apoptosis pathway. *Biochem Biophys Res Commun* **475**: 37–43.

Hoppe G, Yoon S, Gopalan B, Savage AR, Brown R, Case K, Vasanji A, Chan ER, Silver RB, Sears JE (2016) Comparative systems pharmacology of HIF stabilization in the prevention of retinopathy of prematurity. *Proc Natl Acad Sci USA* **113**: E2516–E2525.

Iansante V, Choy PM, Fung SW, Liu Y, Chai JG, Dyson J, Del Rio A (2015) PARP14 promotes the Warburg effect in hepatocellular carcinoma by inhibiting JNK1-dependent PKM2 phosphorylation and activation. *Nat Commun* **6**: 7882.

Jain IH, Zazzeron L, Goli R, Alexa K, Schatzman-Bone S, Dhillon H, Goldberger O, Peng J, Shalem O, Sanjana NE, Zhang F, Goessling W, Zapol WM, Mootha VK (2016) Hypoxia as a therapy for mitochondrial disease. *Science* **352**: 54–61.

Jeong MH, Jin YH, Kang EY, Jo WS, Park HT, Lee JD, Yoo YJ, Jeong SJ (2004) The modulation of radiation-induced cell death by genistein in K562 cells: activation of thymidine kinase 1. *Cell Res* **14**: 295–302.

Kurahashi N, Iwasaki M, Inoue M, Sasazuki S, Tsugane S (2008) Plasma isoflavones and subsequent risk of prostate cancer in a nested case-control study: the Japan Public Health Center. *J Clin Oncol* **26**: 5923–5929.

Li S, Wu L, Feng J, Li J, Liu T, Zhang R, Xu S, Cheng K, Zhou Y, Zhou S, Kong R, Chen K, Wang F, Xia Y, Lu J, Zhou Y, Dai W, Guo C (2016) *In*

vitro and *in vivo* study of epigallocatechin-3-gallate-induced apoptosis in aerobic glycolytic hepatocellular carcinoma cells involving inhibition of phosphofructokinase activity. *Sci Rep* **6**: 28479.

Lis P, Dylag M, Niedzwiecka K, Ko YH, Pedersen PL, Goffeau A, Ulaszewski S (2016) The HK2 dependent 'Warburg effect' and mitochondrial oxidative phosphorylation in cancer: Targets for effective therapy with 3-bromopyruvate. *Molecules* **21**: pii: E1730.

Liu T, Singh R, Rios Z, Bhushan A, Li M, Sheridan PP, Bearden SE, Lai JC, Agbenowu S, Cao S, Daniels CK (2015) Tyrosine phosphorylation of HSC70 and its interaction with RFC mediates methotrexate resistance in murine L1210 leukaemia cells. *Cancer Lett* **357**: 231–241.

Mazure NM (2017) VDAC in cancer. *Biochim Biophys Acta* **1858**: 665–673.

Mueckler M, Thorens B (2013) The SLC2 (GLUT) family of membrane transporters. *Mol Aspects Med* **34**: 121–138.

Qin J, Chen JX, Zhu Z, Teng JA (2015) Genistein inhibits human colorectal cancer growth and suppresses miR-95, Akt and SGK1. *Cell Physiol Biochem* **35**: 2069–2077.

Semenza GL (2013) HIF-1 mediates metabolic responses to intratumoral hypoxia and oncogenic mutations. *J Clin Invest* **123**: 3664–3671.

Shen YC, Ou DL, Hsu C, Lin KL, Chang CY, Lin CY, Liu SH, Cheng AL (2013) Activating oxidative phosphorylation by a pyruvate dehydrogenase kinase inhibitor overcomes sorafenib resistance of hepatocellular carcinoma. *Br J Cancer* **108**: 72–81.

Shike M, Doane AS, Russo L, Cabal R, Reis-Filho JS, Gerald W, Cody H, Khanin R, Bromberg J, Norton L (2014) The effects of soy supplementation on gene expression in breast cancer: a randomized placebo-controlled study. *J Natl Cancer Inst* **106**.

Vander Heiden MG, Cantley LC, Thompson CB (2009) Understanding the Warburg effect: the metabolic requirements of cell proliferation. *Science* **324**: 1029–1033.

Vera JC, Reyes AM, Carcamo JG, Velasquez FV, Rivas CI, Zhang RH, Strobel P, Iribarren R, Scher HI, Slebe JC, Golde DW (1996) Genistein is a natural inhibitor of hexose and dehydroascorbic acid transport through the glucose transporter, GLUT1. *J Biol Chem* **271**: 8719–8724.

Wang SD, Chen BC, Kao ST, Liu CJ, Yeh CC (2014) Genistein inhibits tumor invasion by suppressing multiple signal transduction pathways in human hepatocellular carcinoma cells. *BMC Compl Altern Med* **14**: 26.

Wang YX, Tian K, He CC, Ma XL, Zhang F, Wang HG, An D, Heng B, Jiang YG, Liu YQ (2017) Genistein inhibits hypoxia, ischemic-induced death, and apoptosis in PC12 cells. *Environ Toxicol Pharmacol* **50**: 227–233.

Wu CH, Ho YS, Tsai CY, Wang YJ, Tseng H, Wei PL, Lee CH, Liu RS, Lin SY (2009) *In vitro* and *in vivo* study of phloretin-induced apoptosis in human liver cancer cells involving inhibition of type II glucose transporter. *Int J Cancer* **124**: 2210–2219.

Xu L, Ding Y, Catalona WJ, Yang XJ, Anderson WF, Jovanovic B, Wellman K, Killmer J, Huang X, Scheidt KA, Montgomery RB, Bergan RC (2009) MEK4 function, genistein treatment, and invasion of human prostate cancer cells. *J Natl Cancer Inst* **101**: 1141–1155.

Zhang H, Gao P, Fukuda R, Kumar G, Krishnamachary B, Zeller KI, Dang CV, Semenza GL (2007) HIF-1 inhibits mitochondrial biogenesis and cellular respiration in VHL-deficient renal cell carcinoma by repression of C-MYC activity. *Cancer Cell* **11**: 407–420.

Zhang X, Cook KL, Warri A, Cruz IM, Rosim M, Riskin J, Helferich W, Doerge D, Clarke R, Hilakivi-Clarke L (2017) Lifetime genistein intake increases the response of mammary tumors to tamoxifen in rats. *Clin Cancer Res* **23**: 814–824.

Zhou J, Liu Y (2013) Effects of genistein and estrogen on the genioglossus in rats exposed to chronic intermittent hypoxia may be HIF-1alpha dependent. *Oral Dis* **19**: 702–711.